

RESEARCH

Open Access



Characteristics and clinical value of intestinal metabolites in 4 to 6-year-old children with OSAHS

Yanbo Lu¹, Daina Chen¹, Junhua Wu^{1*} and Jishan Zheng^{1*}

Abstract

Objective This study aims to explore the characteristics and functional changes of intestinal metabolites in children with obstructive sleep apnea hypopnea syndrome (OSAHS) aged 4–6 years old through metabolomic approaches, screen potential biomarkers and analyze their correlation with clinical indicators and preliminary discuss the roles of intestinal metabolites in the occurrence and development of OSAHS.

Methods We collected fecal samples from 40 OSAHS children and 40 healthy controls aged 4–6 years and recorded some OSAHS-related clinical indicators. Fecal specimens were used to detect all metabolites through untargeted metabolomics.

Results This study identified a total of 1164 intestinal metabolites and screened out 254 differential metabolites. In the OSAHS group, the relative content of 96 metabolites were higher than the control group, while the relative content of 158 metabolites were lower. The receiver operating characteristic curve analysis results showed that the area under the curve of 14 differential metabolites was greater than 0.8. The area under the curve of Formononetin is the highest, at 0.9100, with sensitivity and specificity of 82.5% and 90.0%, respectively, and is positively correlated with OAHl. The differential metabolite functions mainly include the metabolism of fatty acids and other lipid substances, cellular signaling, protein and amino acid related metabolism, disease-related functions, glucose metabolism, and vitamin metabolism.

Conclusion The intestinal metabolites and metabolic function of 4-to-6-year-old children with OSAHS altered. There was a correlation between differential metabolites and clinical indicators such as uric acid, hemoglobin, and blood sugar, which has potential diagnostic value for OSAHS screening.

Keywords Obstructive sleep apnea hypopnea syndrome, Children, Intestinal metabolite, Biomarker

*Correspondence:

Junhua Wu
wudata@163.com
Jishan Zheng
zjs222@163.com

¹The Affiliated Women and Children's Hospital of Ningbo University,
Liuting Street 339, Ningbo City, Zhejiang Province 315012, China



© The Author(s) 2025. **Open Access** This article is licensed under a Creative Commons Attribution-NonCommercial-NoDerivatives 4.0 International License, which permits any non-commercial use, sharing, distribution and reproduction in any medium or format, as long as you give appropriate credit to the original author(s) and the source, provide a link to the Creative Commons licence, and indicate if you modified the licensed material. You do not have permission under this licence to share adapted material derived from this article or parts of it. The images or other third party material in this article are included in the article's Creative Commons licence, unless indicated otherwise in a credit line to the material. If material is not included in the article's Creative Commons licence and your intended use is not permitted by statutory regulation or exceeds the permitted use, you will need to obtain permission directly from the copyright holder. To view a copy of this licence, visit <http://creativecommons.org/licenses/by-nc-nd/4.0/>.

Introduction

Obstructive sleep apnea hypopnea syndrome (OSAHS) is a syndrome of chronic intermittent hypoxia (IH), hypercapnia and sleep fragmentation (SF), which is secondary to a series of pathophysiological changes [1]. The incidence rate of OSAHS in children is 1.2%~13% [2–3]. Adenoid and/or tonsil hypertrophy is the main cause of OSAHS in children [4]. OSAHS can occur in all ages, of which the most obvious clinical symptoms and surgical interventions (tonsillectomy and adenoidectomy) are mainly concentrated in 4 to 6 years old, mainly because of adenoid and/or tonsil in children of this age, which accounts for the largest proportion of upper airway volume [5, 6]. Research has shown that children with OSAHS who have not been diagnosed and treated in a timely manner are associated with adenoid facial features, neurocognitive impairment, learning disabilities, behavioral abnormalities, developmental delays, drowsiness, and abnormal secretion of sex hormones [6]. Therefore, early diagnosis and treatment of OSAHS in children is crucial.

Polysomnography (PSG) conducted in a sleep laboratory is the standard method for diagnosing OSAHS [7]. Due to the time-consuming and laborious nature of PSG, it cannot be used for large-scale screening in clinical practice. It is urgent to replace screening methods to identify OSAHS, so that children can receive standardized medical treatment and sufficient attention as soon as possible.

The increase in oxidative stress and inflammatory activation caused by IH and SF is the main pathophysiological mechanism of OSAHS, which is related to cardiovascular disease, cognitive impairment, and metabolic syndrome. Numerous studies have explored potential biomarkers of OSAHS [8, 9]. However, the existing research has several shortcomings. The first is the problem of insufficient sample size; The second is that some studies only included the study subjects into the experimental group based on clinical symptoms or questionnaire surveys, that is, OSAHS was not diagnosed through the gold standard PSG; The third reason is that the specificity, sensitivity, or diagnostic value of biomarker screening diagnosis is not high. Therefore, it is necessary to find more efficient and economical screening and diagnostic methods for OSAHS in children.

Recent studies have shown an important connection between OSAHS and gut microbiota [10–14]. Changes in gut microbiota have been observed in both OSAHS animal models and adult and child OSAHS patients, including changes in microbial diversity [10–13], imbalance in the proportion of Firmicutes to Bacteroidetes (considered a characteristic microecological change of obesity) [10, 12], decreased microbiota producing short chain fatty acids (SCFAs) [11, 13, 14], and increased

pro-inflammatory strains [13, 14]. IH, SF and oxidative stress leads to intestinal microbiota imbalance, leading to local inflammation and changes in intestinal permeability, further exacerbating systemic inflammatory reactions [15]. One study revealed that an enrichment of arachidonic acid, docosahexaenoic acid, and 11Z-eicosenoic acid and reduction in stearic acid, 5-hydroxyindoleacetic acid, gluconic acid, and α -hydroxydeoxycholic acid were observed in intestinal metabolites in adult OSAHS patients [16].

However, there is few researches on intestinal metabolites related to OSAHS in children. Therefore, we hope to explore the characteristics of intestinal metabolites in children with OSAHS through intestinal metabolomics analysis, screen for possible biomarkers and evaluate their diagnostic value, and discuss the correlation between intestinal metabolic changes and OSAHS.

Methods

Participants

This study recruited 40 OSAHS children and 40 healthy controls. OSAHS children were participants who complained of snoring in the Otolaryngology or Respiratory Department of Ningbo Women and Children's Hospital from October 2020 to December 2021. The healthy controls were children of hospital colleagues during the same period. All participants have undergone free PSG and recorded indices obstructive apnea/hypopnea index (OAHl) and lowest oxygen saturation ($LaSO_2$). The diagnostic criteria for OSAHS were implemented in accordance with Chinese guideline for the diagnosis and treatment of childhood obstructive sleep apnea (2020) which stated that $OAHl > \text{once per hour}$ [7]. Inclusion criteria: 4-to-6-year-old children with $OAHl > 1$ were included in the case group, while 4-to-6-year-old children with $OAHl \leq 1$ were included in the control group. Exclusion criteria: congenital malformations of airway or digestive tract; diseases that cause chronic hypoxia such as anemia, congenital heart disease, restrictive lung disease and so on; using antibiotics or probiotics within the past 3 months; functional constipation, irritable bowel syndrome and other gastrointestinal diseases; the control group excluded snoring or tonsillar enlargement.

We recorded the general information and clinical indicators of all participants, including age, gender, height, weight, body mass index (BMI), degree of tonsillar enlargement, hemoglobin (Hb), platelets (plt), uric acid (UA), creatinine (Cre), blood urea nitrogen (BUN), blood glucose (Glu), triglycerides (TG) and total cholesterol (TC).

This study complied with the basic principles of the Helsinki Declaration and was approved by the Ethical Committee of Women and Children's Hospital of Ningbo

University, and all participants have obtained informed consent from their guardians.

Sample collecting

We provided guardians with a clean and sterile specimen box and a disposable sterile sampling spoon for collecting the first feces of children after waking up in the morning. Fecal samples (1 g) were collected, avoiding surface and urine contamination, and immediately stored in a freezer at -80°C .

Sample preprocessing

Extraction of metabolites from the samples: (1) add 200 μg fecal samples to a 2mL centrifuge tube containing 600 μL methanol with 4 $\mu\text{g}/\text{mL}$ 2-chloro-L-phenylalanine as internal standard, vortex oscillation for 30 s; (2) add 100 mg grinding beads to a centrifuge tube, grind at 60 Hz for 90 s; (3) ultrasound at room temperature for 10 min; (4) centrifuge at 12,000 rpm at 4°C for 10 min, take the supernatant and pass it through 0.2 μm filter, and add the filtrate to the detection bottle.

Quality control (QC) sample preparation: take 10 μL out of each extracted test sample mixing into QC sample, which is used to correct deviations in the analysis results of mixed samples and errors caused by the analysis instrument's own system. After every 10 samples are tested, QC sample is inserted into the running sequence to monitor the stability of the collected data.

Liquid Chromatography-Mass spectrometry (LC-MS)

LC-MS uses liquid chromatography as the separation system and mass spectrometry as the detection system. The sample is separated from the mobile phase in the chromatographic section. Then the separated fragments are ionized in mass spectrometry and a mass spectrum is obtained for subsequent identification. Liquid chromatographic separations were performed on a Thermo Vanquish ultra efficient liquid phase system (Thermo Fisher Scientific, U.S.A.) equipped with a Waters ACQUITY UPLC[®] HSS T3 column (150 \times 2.1 mm, 1.8 μm). Mass spectrometry operations were performed on a Thermo Orbitrap Exploris 120 mass spectrometer (Thermo Fisher Scientific, U.S.A.) with spray voltages of 3.5 kV in positive ion mode (ESI+) and -2.5 kV in negative ion mode (ESI $-$), respectively.

Data preprocessing and metabolite identification

Raw data were converted to the mzXML file format using the MSConvert tool in the Proteowizard v3.0.8789 software package. RXCMS software package was used for peak detection, peak filtering and peak alignment processing to form a data matrix of retention time, mass-to-charge ratio and peak intensity. For quality assurance, all characteristic peaks in the QC sample with a relative

standard deviation exceeding 30% were removed. We compared the data with reference standards for known chemicals in metabolite databases (including HMDB, massbank, LipidMaps, mzcloud, KEGG) and provide precise metabolite annotations. A total of 1164 metabolites were identified.

Data analysis

The Ropls software was used for multivariate data analyses and models. After scaling data, models were built on orthogonal partial least-square discriminant analysis (OPLS-DA). All the models evaluated were tested for over fitting with methods of permutation tests. R^2 and Q^2 values at the Y-axis intercept must be lower than those of Q^2 and the R^2 of the non-permuted model. OPLS-DA allowed the determination of discriminating metabolites using the variable importance on projection (VIP). The P value, VIP value produced by OPLS-DA and fold change (FC) were applied to discover the contributable-variable for classification. Finally, P value < 0.05 and VIP values > 1 were considered to be statistically significant metabolites.

Differential metabolites were subjected to pathway analysis by MetaboAnalyst. The identified metabolites in metabolomics were then mapped to the KEGG pathway for biological interpretation of higher-level systemic functions. The metabolites and corresponding pathways were visualized using KEGG Mapper tool.

Statistical analysis

In this study, SPSS 22.0 and GraphPad Prism8 software were used for statistical analysis. Independent sample t-tests were performed for normal continuous data, which were presented with mean \pm SD. The hierarchical classification data is compared using chi square test. The diagnostic value of differential metabolites was evaluated using Receiver Operating Characteristic (ROC) curves. The correlation between differential metabolites and clinical indicators used Spearman correlation. All results with $P < 0.05$ indicate significant differences.

Results

General characteristics of the participants

There was no difference in general characteristics between the two groups, including age, gender, height, weight, BMI, and blood pressure. Children with OSAHS showed much higher OAH and degree of tonsil enlargement and lower LaSO_2 as compared with controls. No significant difference was detected in other clinic parameters (Hb, plt, TG, UA, Cre, BUN, Glu, TC) between groups. All specific characteristics is shown in Table 1.

Table 1 Baseline clinical characteristics of the participants

		OSAHS (n = 40)	Controls (n = 40)	t/ χ^2	P
Gender (male/female)		23/17	20/20	0.453	0.501
Age (years)		5.169 ± 0.619	3.985 ± 0.640	1.302	0.197
Height (cm)		111.450 ± 7.002	110.538 ± 5.620	0.643	0.522
Weight (kg)		20.782 ± 4.903	19.380 ± 2.936	1.547	0.126
BMI (kg/m ²)		16.656 ± 2.725	15.828 ± 1.787	1.599	0.114
SBP (mmHg)		103.925 ± 8.260	104.525 ± 9.863	-0.295	0.769
DBP (mmHg)		61.600 ± 11.542	61.725 ± 7.786	-0.057	0.955
Degree of tonsil enlargement	No	0	40	80.000	< 0.0001
	I	4	0		
	II	8	0		
	III	28	0		
OAHl (times/hour)		7.886 ± 4.188	0.175 ± 0.128	11.639	< 0.0001
LaSO ₂ (%)		76.925 ± 11.032	90.700 ± 3.495	-7.528	< 0.0001
Hb (g/L)		127.182 ± 6.483	126.533 ± 9.387	0.278	0.782
plt (10 ⁹ /L)		313.212 ± 74.404	328.400 ± 74.627	-0.655	0.516
TG (mmol/L)		1.237 ± 0.545	1.155 ± 0.765	0.444	0.659
UA (μmol/L)		244.719 ± 55.855	250.000 ± 70.647	-0.296	0.769
Cre (μmol/L)		49.688 ± 4.862	49.842 ± 7.112	-0.092	0.927
BUN (mmol/L)		5.138 ± 1.066	4.608 ± 0.738	1.907	0.062
Glu (mmol/L)		5.187 ± 0.550	5.101 ± 0.844	0.443	0.660
TC (mmol/L)		4.677 ± 0.793	4.335 ± 0.621	1.608	0.114

BMI = body mass index, SBP = systolic blood pressure, DBP = diastolic blood pressure, OAHl = obstructive apnea/hypopnea index, Hb = hemoglobin, plt = platelet, TG = triglyceride, UA = uric acid, Cre = blood creatinine, BUN = blood urea nitrogen, Glu = glucose, TC = total cholesterol

Orthogonal partial least squares discriminant analysis

The OPLS-DA displacement test chart (Fig. 1A, B) showed that in both positive and negative ion modes, all blue Q2 points are lower than the original blue Q2 point on the far right, and the intersection point of the Q2 point regression line and the ordinate is less than the zero, indicating that the results of model established by OPLS-DA were reliable and effective.

The OPLS-DA score chart (Fig. 1C, D) showed that under positive and negative ion modes in LC-MS, the majority of samples were within the 95% confidence interval. The clustering differentiation between the two groups of samples was relatively significant. The evaluation indicators of the model in the positive ion mode were $R^2X = 0.217$, $R^2Y = 0.983$, $Q^2 = 0.843$, with the horizontal axis explaining 3.3% of the difference and the vertical axis explaining 14.5% of the difference; In the negative ion mode, the model evaluation indicators $R^2X = 0.215$, $R^2Y = 0.988$, $Q^2 = 0.848$, with the horizontal axis explaining 3.5% of the difference and the vertical axis explaining 14.9% of the difference. The above results indicated that the model had good fitting and predictive ability, indicating a potential difference in the composition of metabolites between the two groups of samples.

Overall characteristics of metabolites

This study identified a total of 1164 metabolites, including 14 amino acids, 7 benzene ring compounds, 6 fatty acids, 6 organic acids and derivatives, 4 purine and

pyrimidine derivatives, 4 organic nitrogen compounds, 2 alkaloids and derivatives, 2 amine substances, 2 organic oxygen compounds, and 3 unclassified substances in the top 50 overall relative content (Fig. 2A).

Metabolites with significant differences between the two groups

The screening criteria for differential metabolites were that the P-value of the Mann-Whitney-Wilcoxon-Test was less than 0.05, and the Variable Importance in the Projection (VIP) of the OPLS-DA first principal component variable was greater than 1. Out of 1164 metabolites, a total of 254 differential metabolites were screened, with 96 metabolites in the OSAHS group showing an increase and 158 metabolites showing a decrease in relative content (Fig. 2B).

According to the analysis results of fold change (FC) value, the five differential metabolites with the highest FC value were 3,4-Dihydroxymandelic acid (DHMA), Triethanolamine, Loperamide, Stearidonic acid, and Formononectin while the five differential metabolites with the lowest FC value were Alantolactone (Ala), Deoxycholic acid, Isoferulic acid, Mitomycin, and D-β-Phenylalanine (Table 2).

Correlation analysis between metabolites with the most significant differences and clinical indicators

We conducted a correlation analysis between the 10 metabolites with the most significant differences

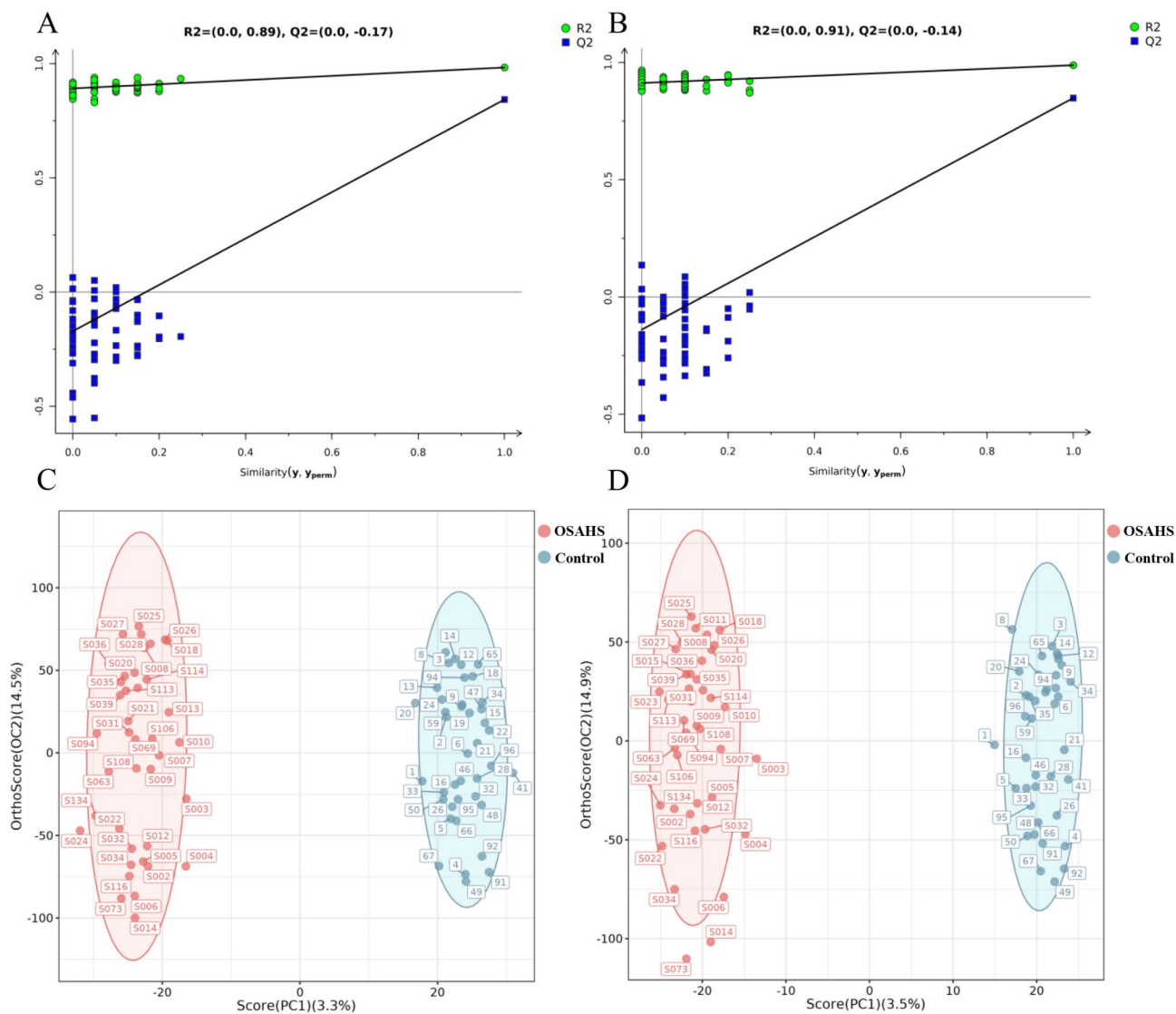


Fig. 1 Orthogonal Partial Least Squares Discriminant Analysis. **(A)** Positive ion Mode OPLS-DA Permutation Test Chart; **(B)** Negative ion mode OPLS-DA displacement test chart; **(C)** Positive ion mode OPLS-DA score map; **(D)** Negative ion mode OPLS-DA score chart

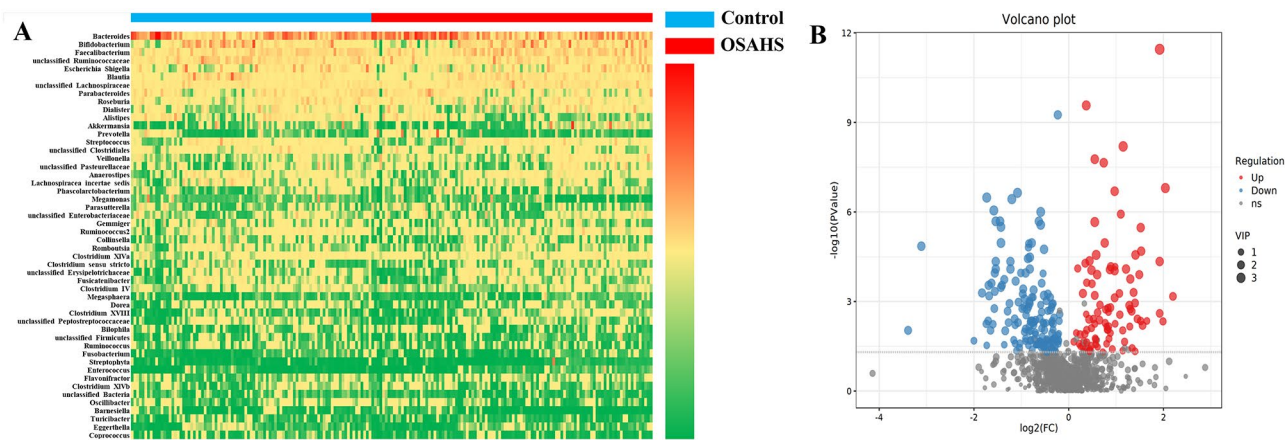


Fig. 2 Overall distribution of metabolites (A) Heatmap of top 50 metabolites in content; (B) Volcano Plot of metabolites distribution

Table 2 10 Metabolites with the most significant difference FC value

Differential Metabolites	FC	mz	OSAHS	Control	P value
3,4-Dihydroxy-mandelic acid	4.58	183.03	4310635.62	941137.75	0.0007
Triethanol-amine	4.12	132.1	3,976,874,999	966137742.6	< 0.0001
Loperamide	3.96	477.23	22799614.2	5753957.47	0.0046
Stearidonic acid	3.80	277.22	127,053,311	33468654.04	0.0025
Formononectin	3.79	267.07	17757161.3	4691414.58	< 0.0001
Alantolactone	0.10	233.15	5432792.37	56803767.88	0.0093
Deoxycholic acid	0.12	392.3	4,880,487,917	42,086,369,684	< 0.0001
Isoferulic acid	0.25	177.05	3316069.29	13272322.57	0.0206
Mitomycin	0.28	335.13	9186872.64	32587250.9	0.0005
D-β-Phenylalanine	0.30	166.09	125,478,540	414859391.4	< 0.0001

mz: Mass-to-charge ratio

in Results 3.4 and the clinical indicators related to OSAHS. The five positive correlation results were as follows: 3,4-Dihydroxymandelic acid with UA ($r=0.489$, $P=0.005$), Loperamide with Hb ($r=0.478$, $P=0.005$), Formononectin with OAH1 ($r=0.331$, $P=0.037$), Isoferulic acid with OAH1 ($r=0.334$, $P=0.035$), and Mitomycin with Hb ($r=0.382$, $P=0.028$). The three negative correlation results were as follows: Loperamide with LaSO_2 ($r=-0.375$, $P=0.017$), Stearidonic acid with Glu ($r=-0.351$, $P=0.049$), and Alantolactone with LaSO_2 ($r=-0.328$, $P=0.039$), as shown in Fig. 3.

Diagnostic value of differential metabolites

We conducted ROC curve analysis on all 254 differential metabolites, and there were a total of 14 metabolites with area under curve (AUC) greater than 0.8, as shown in Table 3; Fig. 4. Among them, the AUC of the Formononectin was the highest, at 0.9100, with sensitivity and specificity of 82.5% and 90.0%, respectively. In addition, L-Prolinamide, Cysteine-S-sulfate, Epsilon-caprolactam, 4-Methoxybenzaldehyde, 1,1-Dimethylbiguanide, Cybutryne, Serotonin and D-Arabitol had potential diagnostic value (specificity>85%); L-Prolinamide, Cysteine-S-sulfate, 20a,22b-Dihydroxycholesterol, Triethanolamine, D-beta-Phenylalanine and Oxoglutaric acid had potential screening value (sensitivity>85%).

Functional analysis of differential metabolites

We compared 254 differential metabolites with KEGG database metabolic pathways and matched a total of 113 related metabolic functional pathways (Fig. 5A), which included 27 functions related to fatty acids and other lipid substances (Table S1), 19 functions related to cell signal transduction (Table S2), 18 functions related to

protein and amino acid metabolism (Table S3), 18 functions related to diseases (Table S4), 8 functions related to glucose metabolism (Table S5), 6 functions related to vitamin metabolism (Table S6), and 18 functions related to other metabolism (Table S7).

Enrichment analysis showed that the top 20 metabolic pathways with the lowest P-value (the most significant impact of detected differential metabolites on this pathway) were Lysine degradation, Vitamin digestion and absorption, Rheumatoid arthritis, Central carbon metabolism in cancer, Protein digestion and absorption, mTOR signaling pathway, Alanine, aspartate and glutamate metabolism, Steroid hormone biosynthesis, Basal cell carcinoma, and Arginine biosynthesis, as shown in Fig. 5B. The differential metabolites involved in the main metabolic pathways were shown in a network diagram (Fig. 6).

Discussion

This study analyzed the gut metabolome of children with OSAHS, finding that OSAHS children had characteristic changes in gut metabolites and metabolic pathways. The differential metabolites screened have high diagnostic value and are related to the severity of OSAHS, which may become biomarkers for clinical screening and diagnosis of OSAHS. The degree of tonsil enlargement and OAH1 in OSAHS children were significantly higher than the controls, while LaSO_2 was significantly lower than that in the control group, which was consistent with the related manifestations of OSAHS disease. Despite the differences these disease indicators, there weren't any significant differences in the other attributes between the two groups. In fact, obesity is one of the important risk factors for OSAHS. The deposition of fat around the pharynx can exacerbate respiratory stenosis; Abdominal fat deposition leads to decreased lung capacity; Adipose cell hypertrophy increases the diffusion distance between capillaries and adipose tissue cells, leading to tissue hypoxia by activating the nuclear factor kappa β (NF- κ B) and hypoxia inducible factor (HIF)-1 α inducing systemic inflammation [17]. Several large-scale studies have concluded that weight gain was associated with an increase in the prevalence and severity of OSAHS [18–20]. In this study, the weight and BMI of OSAHS children were slightly higher than those in the control group, but statistical differences were not attained, which was consistent with the results of Valentini's research [10]. This might be related to the sample size. In addition, it also indicated that OSAHS is the result of the interaction of multiple factors, including obesity, neuromuscular abnormalities, activation of inflammatory mediator cascade, neurodegenerative diseases and anatomical disorders [1].

There was no significant difference in clinical indicators between the two groups. OSAHS is associated with

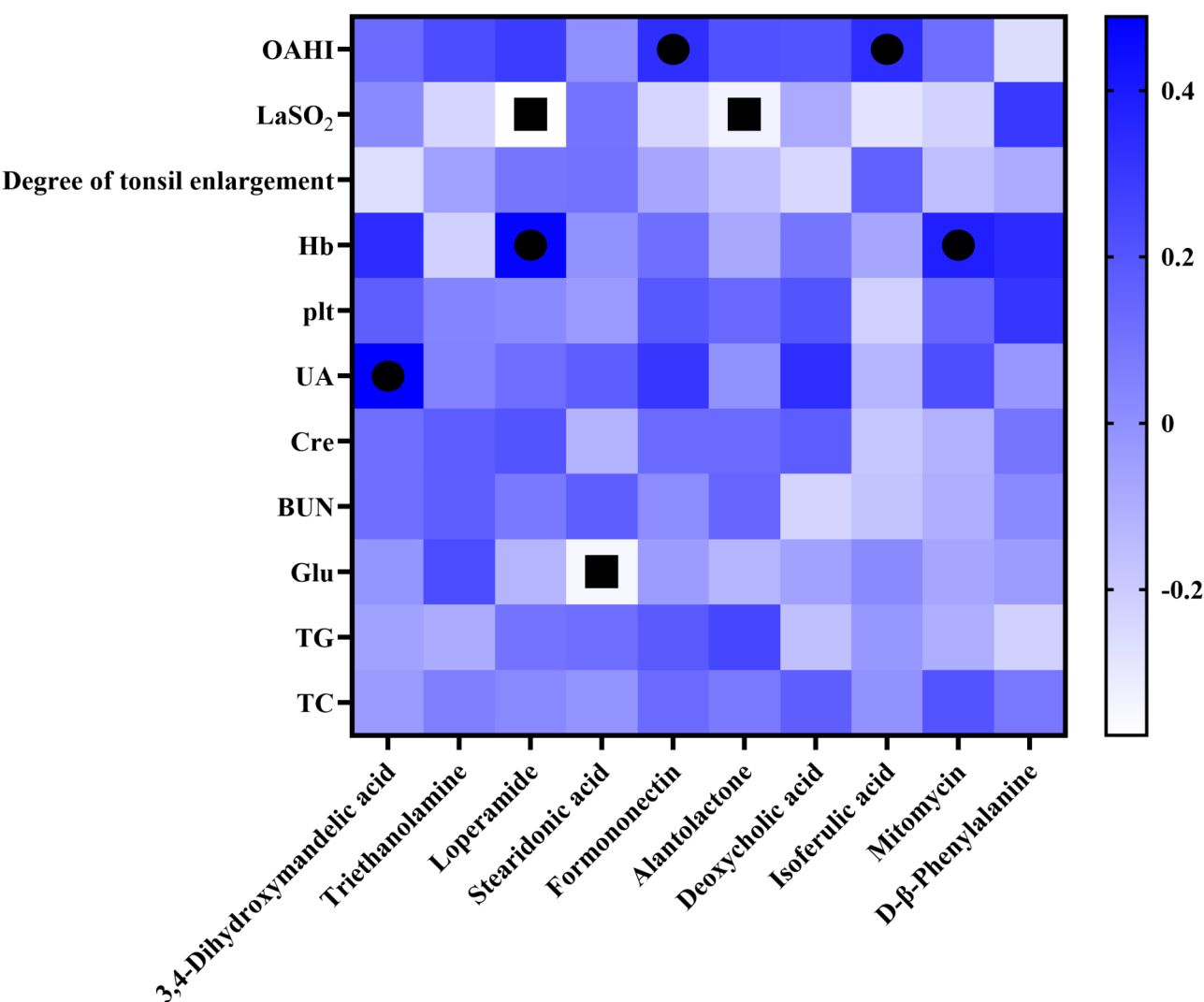


Fig. 3 Heatmap of correlation analysis between differential metabolites and clinical indicators; ●: positive correlation, ■: negative correlation

Table 3 Table of 14 metabolites with the highest AUC

metabolites	FC	P value	AUC	Sensitivity(%)	Specificity(%)	95% CI
Formononectin	3.79	<0.0001	0.9100	82.5	90.0	0.8459–0.9741
L-Prolinamide	1.29	<0.0001	0.8800	87.5	90.0	0.7891–0.9709
Cysteine-S-sulfate	0.85	<0.0001	0.8740	97.5	85.0	0.7817–0.9670
20a,22b-Dihydroxycholesterol	2.23	<0.0001	0.8544	95.0	70.0	0.7679–0.9414
Epsilon-caprolactam	1.47	<0.0001	0.8456	72.5	97.5	0.7472–0.9440
4-Methoxybenzaldehyde	1.67	<0.0001	0.8431	75.0	100.0	0.7474–0.9389
Triethanolamine	4.12	<0.0001	0.8244	92.5	60.0	0.7372–0.9122
1,1-Dimethylbiguanide	1.96	<0.0001	0.8219	72.5	100.0	0.7165–0.9272
Sulfamethoxypyridazine	0.47	<0.0001	0.8206	77.5	72.5	0.7297–0.9115
D-beta-Phenylalanine	0.30	<0.0001	0.8169	100.0	55.0	0.7243–0.9088
Cybutryne	0.43	<0.0001	0.8156	72.5	85.0	0.7192–0.9121
Oxoglutaric acid	0.33	<0.0001	0.8063	92.5	75.0	0.7026–0.9099
Serotonin	0.66	<0.0001	0.8050	65.0	90.0	0.7077–0.9023
D-Arabitol	2.14	<0.0001	0.8031	62.5	90.0	0.7004–0.9058

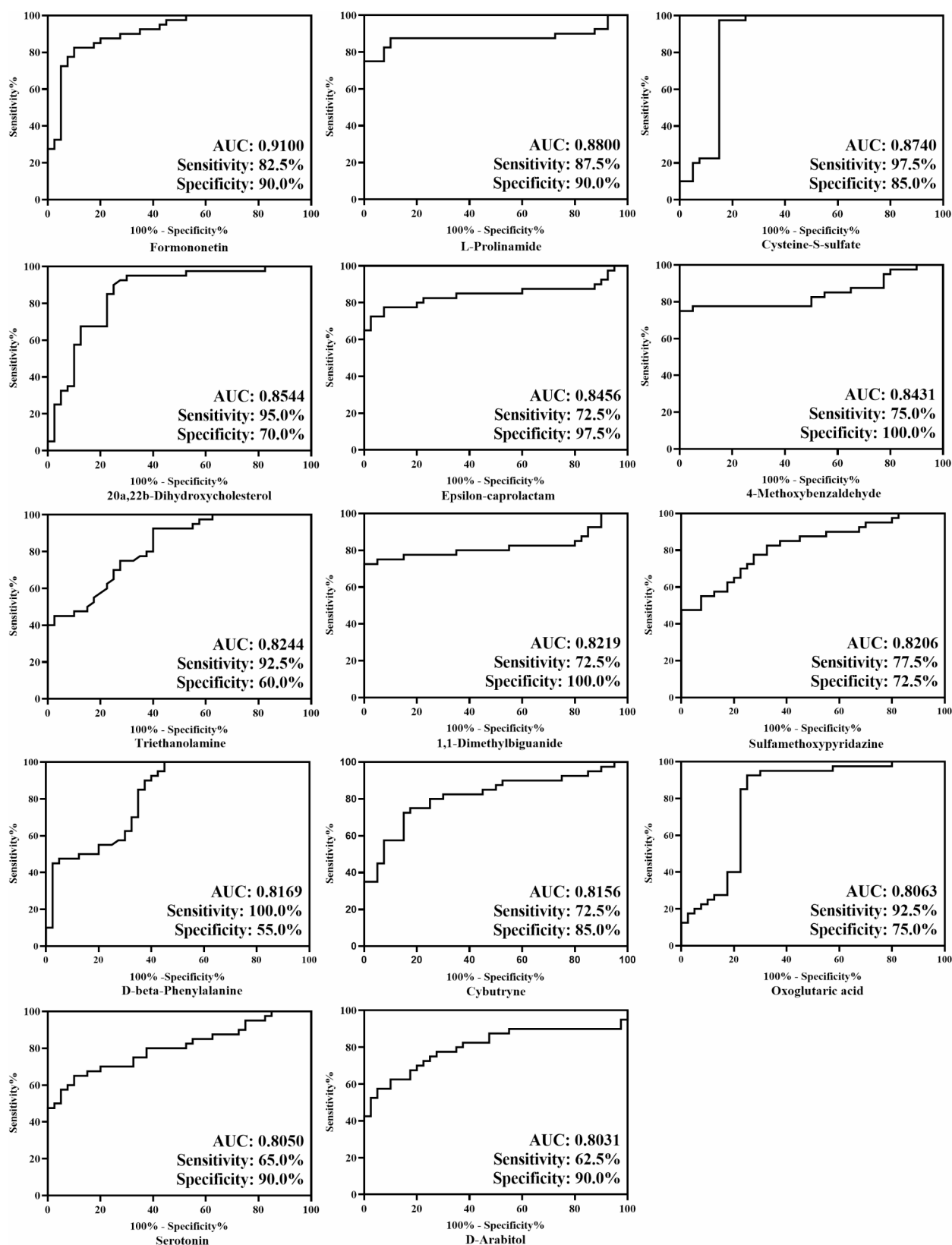


Fig. 4 ROC curves of 14 metabolites with the highest diagnostic value

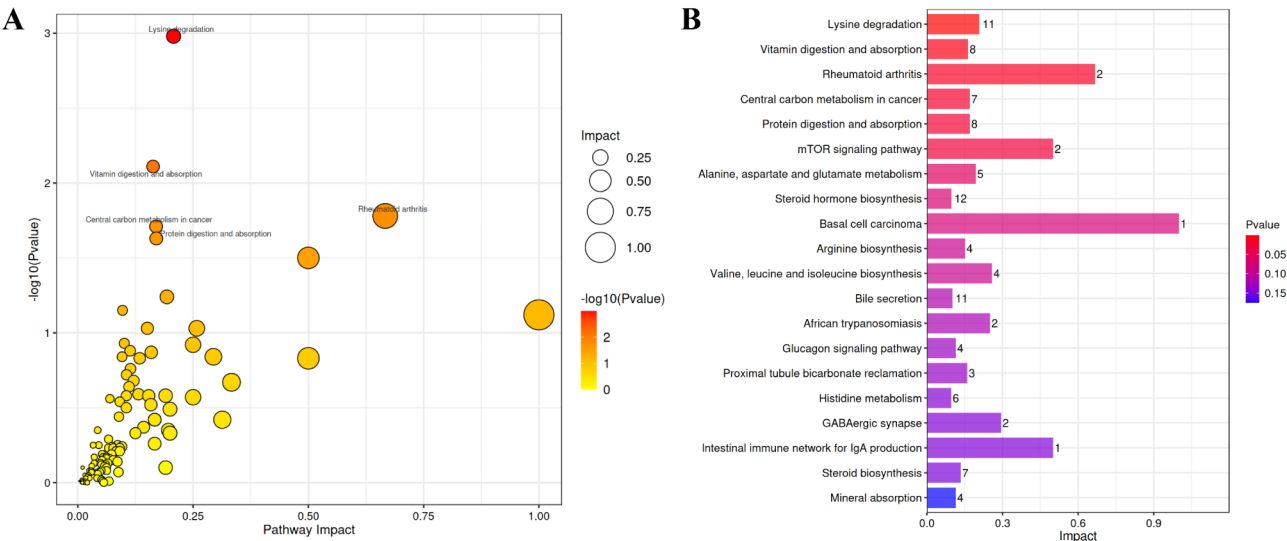


Fig. 5 Differential metabolite related metabolic pathways. **(A)** Bubble diagram of influencing factors of metabolic pathway; **(B)** Histogram of the top 20 metabolic pathway influencing factors with the lowest P value

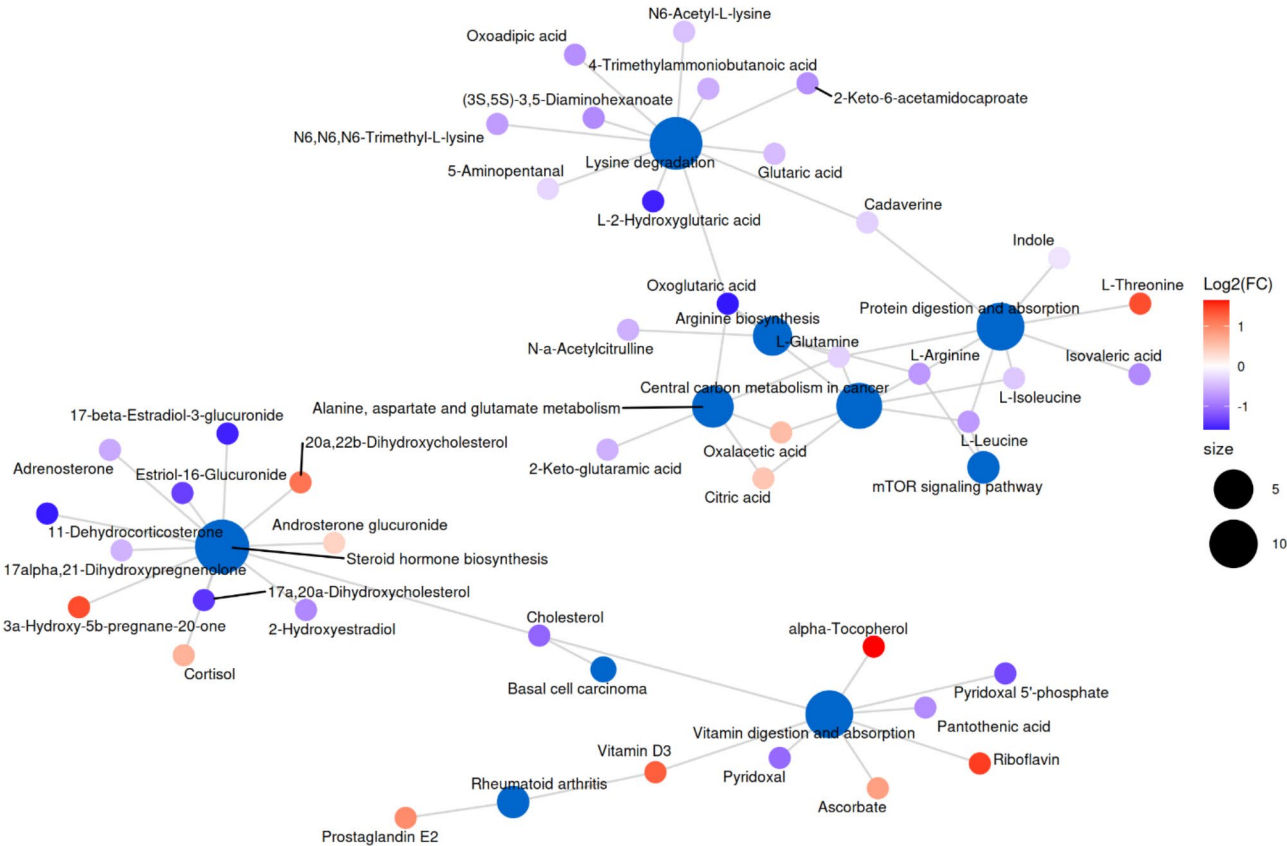


Fig. 6 Metabolic pathway network diagram

cardiovascular and metabolic comorbidities, including hypertension, atherosclerosis, dyslipidemia and insulin resistance [4, 21, 22]. Intermittent hypoxia, sleeping fragment, increased sympathetic nervous activity, enhanced oxidative stress, and systemic inflammation are

hypothesized mechanisms leading to metabolic changes in OSAHS [23]. Prior research had shown that OSAHS was associated with changes in glucose and lipid metabolism, including TC, TG, and Glu [22, 24]. A meta-analysis found that the incidence of polycythemia in OSAHS

patients is about 2%, while continuous positive airway pressure (CPAP) treatment reduces the levels of Hb and hematocrit in OSAHS patients by 4 g/L and 1%, respectively [25]. Shen et al. found that plt in OSAHS children was higher than that in the control group and positively correlated with the severity of OSAHS [26]. Several observational studies have reported a close correlation between OSAHS and serum UA [27, 28]. Previous studies have found that OSAHS patients had varying degrees of renal dysfunction, and UA, Cre, and BUN were all clinical indicators for evaluating renal function [29, 30]. The above indicators have been reported in studies related to OSAHS, but their specific causal relationships were still unclear. In this study, there was no significant difference in the above indicators between the OSAHS group and the control group.

LC-MS identified a total of 1164 small molecule metabolites. The main small molecule substances in intestinal metabolites were amino acids, fatty acids, and organic acids, which were consistent with other metabolomics studies [31]. The result of OPLS-DA showed a significant difference in the overall composition of metabolites between the two groups. A total of 254 differential metabolites were screened out, with 96 metabolites in the OSAHS group increasing in relative content and 158 metabolites decreasing. Among them, amino acids, fatty acids, and bile acids were mainly reduced. It was consistent with previous research, such as a decrease in the microbiota producing SCFAs and the content of intestinal fatty acids and bile acids, changes of microbiota function predicting in purine and amino acid metabolism [11, 13, 14]. SCFAs had a direct anti-inflammatory effect on the intestine, including promoting mucin synthesis, reducing bacterial translocation, maintaining intestinal integrity and alleviating intestinal inflammation [32, 33]. In addition, SCFAs were involved in immunity, adipogenesis, insulin sensitivity, and oxidative stress [34]. The reduction in SCFAs production led to intestinal barrier dysfunction, which may further exacerbate intestinal inflammation.

Through FC analysis, we found that the relative content of DHMA and Triethanolamine were significantly higher than the control group, while the relative content of Ala, Deoxycholic acid and Isoferulic acid were significantly lower. We briefly discuss these differential metabolites and their association with OSAHS in the following paragraphs. DHMA is a metabolite of norepinephrine (NE) formed by bacterial encoded tyramine oxidase and aromatic aldehyde dehydrogenase [35]. A small portion of DHMA is directly produced by the host, while the majority of DHMA in feces is produced by the gut microbiota. NE is abundant in intestinal associated lymphoid tissue, which is the preferred target for initial infection by most intestinal pathogens [36]. The DHMA

produced by gut microbiota from NE can serve as molecular beacons for bacterial pathogens in the intestine, directing them to preferred infection sites and inducing their pathogenicity which may be related to an increase in intestinal pathogens in OSAHS patients. In addition, NE is the main neurotransmitter of the sympathetic nervous system. The pathological mechanism of OSAHS complicated with hypertension has been fully confirmed to be related to sympathetic nervous system hyperactivity. IH increases the expression of HIF, which increases reactive oxygen species (ROS) through HIF-1 dependent activation of pro-oxidase genes and HIF-2 reduction of antioxidant gene transcription. ROS in turn activates the chemical reflex and suppresses the pressure reflex, thereby stimulating the sympathetic nervous system and causing hypertension. Animal models of IH long term indicated that potential mechanisms mediating hypertension include increased sensitivity of chemoreceptors, excessive activity of sympathetic nervous system during the day, excessive production of ROS, and inflammatory effects on resistance vessels [37, 38]. Therefore, DHMA is both a virulence inducer and a chemical inducer, emphasizing the importance of elevated microbial metabolite DHMA from host neurotransmitters as a pathogenic mechanism for intestinal infections and OSAHS.

Triethanolamine is a weakly alkaline organic compound that can react with inorganic or organic acids to form salts. The International Agency for Research on Cancer of the World Health Organization has classified triethanolamine as a Class 3 carcinogen. Mice fed a diet containing 0.3% or 0.03% triethanolamine developed malignant tumors [39]. In recent years, the potential connection between cancer and OSAHS has received attention [18]. The OSAHS animal model indicates that intermittent hypoxia and sleep fragmentation both promote tumor occurrence and changes in tumor malignancy characteristics. Triethanolamine is used as an emulsifier in many cosmetics and topical drugs, which may cause allergic contact dermatitis [40]. Studies have shown that IgE mediated triethanolamine sensitivity leads to refractory sneezing [41]. 28 days of exposure to diethanolamine and triethanolamine resulted in changes in the laryngeal epithelium of rats, including reversible metaplasia at the bottom of the epiglottis, and high concentrations of inflammation extending to the trachea [42]. Another study found that lower concentrations of triethanolamine may be a biostimulant that can promote microbial growth and selectively inhibit fungi and bacteria at higher concentrations [43]. The pathogenic mechanism of triethanolamine mentioned above is consistent with the pathophysiological mechanism of OSAHS. The significant increase of triethanolamine in the feces of children with OSAHS may be related to OSAHS.

Ala is a terpenoid compound that can be isolated from herbaceous plants in the Asteraceae family. Its pharmacological effects include antibacterial, antifungal, antiviral, anti-inflammatory, neuroprotective, and anti-tumor effects [44]. Ala exhibits good antibacterial activity against common human pathogens such as *Staphylococcus aureus*, *Pseudomonas aeruginosa*, *Bacillus cereus*, *Shigella dysenteriae*, and *Mycobacterium tuberculosis* [45–47]. One of Ala's most important pharmacological effects is anti-inflammatory activity, which has been demonstrated in cellular and animal inflammation models [44, 48]. Ala can inhibit NF- κ B and MAPK (a group of serine threonine protein kinases that can be activated by different extracellular stimuli such as cytokines, cell stress, and cell adhesion), reduce IL-1 β , IL-6 and TNF- α proinflammatory cytokines, have potential therapeutic effects in chronic obstructive pulmonary disease, diabetes, rheumatoid arthritis, atopic dermatitis and neuritis related to traumatic brain injury and ischemia/reperfusion injury. In addition, Ala has been proven to have a certain promoting effect on glucose and lipid metabolism. In adipocytes, 1 μ M ALa can improve the decrease in glucose uptake and increase in fat accumulation caused by palmitic acid esters [49]. In L6 myoblasts, Ala can reverse the dysregulation of glucose uptake and insulin resistance caused by long-term exposure to IL-6 [50]. In L02 liver cells, Ala may reduce the lipid deposition of oxidized low-density lipoprotein on liver cells by inhibiting the phosphorylation of a transcriptional regulatory protein STAT3, thereby downregulating the expression of apolipoprotein C3, which is closely related to cardiovascular disease and several metabolic diseases [51]. Ala not only regulates glucose and lipid metabolism, but also has neuroprotective effects by reducing oxidative stress and inflammatory responses [52]. Ala exerts anti-tumor effects through various mechanisms such as inducing endogenous cell apoptosis, oxidative stress, endoplasmic reticulum stress, cell cycle arrest, inhibition of autophagy, and STAT3 phosphorylation [44]. Given the pharmacological effects of Ala mentioned above, further research and exploration are needed to explore the relationship between the reduction of intestinal Ala in children with OSAHS and OSAHS.

Deoxycholic acid is a free bile acid derived from bile acid by removing one oxygen atom. The gut microbiota undergoes various biological transformations of bile acids through biosynthesis and metabolism. Bile acids are responsible for intestinal lipid digestion and act as key nutritional signaling molecules [53]. The regulation of blood lipids, especially cholesterol, is partially achieved through the synthesis and excretion of bile acids into the gastrointestinal tract. The reduction of bile acids excreted into the intestine in children with OSAHS may be related to lipid metabolism disorders and obesity.

Isoferulic acid is a naturally occurring derivative of cinnamic acid, which is the main component of the Chinese herbal medicine Da San Ye Cheng Ma [54]. It is often used as an anti-inflammatory drug in traditional Chinese medicine. Isoferulic acid has anti-inflammatory, antioxidant, antiviral and anti-diabetes properties. Previous research showed that IFA could inhibit the production of macrophage inflammatory protein-2 and inflammatory factor IL-8 [55, 56]. Numerous studies have shown that isoferulic acid has an anti-hyperglycemic effect, reducing blood sugar by inhibiting hepatic gluconeogenesis and increasing glucose utilization in peripheral tissues [57, 58]. Diabetes is a common complication of OSAHS patients. IH induces glucose metabolism disorder, while diabetes neuropathy can affect respiratory central control and upper airway nerve reflex, worsen sleep breathing disorder, and there is a two-way relationship between the two [59]. From the functional characteristics of these five substances, there is a potential correlation with the pathological and physiological mechanisms and related complications of OSAHS. However, this study is limited to the observational stage and requires further cell or animal experiments for verification.

ROC curve analysis was performed on all 254 differential metabolites, and the results showed that the area under the curve of formononetin was the highest, 0.9100, with sensitivity and specificity of 82.5% and 90.0%, respectively. Formononetin was positively correlated with OAH1, which can evaluate the severity of OSAHS and serve as a potential biomarker for OSAHS. Formononetin from prickly stems is a flavonoid compound that exists in various plants such as astragalus, licorice, and red clover. Its proven effects include osteogenesis, neuroprotection, antibacterial, anticancer, and antihypertensive effects [60]. It is known that it is absorbed in the intestine, distributed into tissues through plasma, and excreted by the gallbladder and kidneys. This study found that the loss of formononetin from the intestine in children with OSAHS was significantly higher than that in healthy children, and the specific mechanism needs to be explored. In addition to formononetin, there are 13 differential metabolites with an area under the curve greater than 0.8. The 14 differential metabolites discovered in this study may serve as biomarkers for screening and diagnosis of OSAHS, but they need to be validated in larger cohorts.

The 254 differential metabolites involved a total of 113 metabolic pathways, including 27 fatty acid and other lipid related functions, 19 cell signaling related functions, 18 protein and amino acid related metabolism, 18 disease related functions, 8 sugar metabolism related functions, 6 vitamin metabolism related functions, and 18 other metabolic related functions. The metabolic changes of OSAHS included fatty acid, amino

acid, sugar metabolism, vitamin metabolism. Therefore, the functional prediction of differential metabolites was consistent with previous OSAHS related studies, mainly involving changes in glucose and lipid metabolism and amino acid metabolism [11, 13].

This study provided a potential foundation for the pathological and physiological mechanisms of childhood OSAHS, but it still needs to be validated through experimental research. Of course, this study had several limitations. Firstly, the sample size of this study was limited, and the experimental results need to be validated in more central and large sample cohorts in the future. Secondly, whether changes in gut microbiota in children with OSAHS caused changes in gut metabolites and metabolic pathways, or changes in metabolomics led to changes in gut microbiota in OSAHS patients, as well as the specific relationship between the internal network and the host immune system, still needs further research. In addition to gut metabolomics and gut microbiota, our research group will continue to conduct in-depth research on gut fungi and gut virus, analyze the entire gut microbiota system of OSAHS patients, and supplement objective data on the impact of gut microbiota on the occurrence and development of OSAHS.

Abbreviations

Ala	Alantolactone
AUC	Area Under Curve
BMI	Body Mass Index
BUN	Blood Urea Nitrogen
CPAP	Continuous Positive Airway Pressure
Cre	Creatinine
DHMA	3,4-Dihydroxymandelic acid
FC	Fold Change
Glu	Glucose
Hb	Hemoglobin
HIF	Hypoxia inducible factor
IH	Intermittent Hypoxia
LaSO2	Lowest Oxygen Saturation
LC-MS	Liquid Chromatography-Mass Spectrometry
NF- κ B	Nuclear factor kappa β
OAHl	Obstructive Apnea/Hypopnea Index
OPLS-DA	Orthogonal Partial Least Squares Discriminant Analysis
OSAHS	Obstructive Sleep Apnea Hypopnea Syndrome
Plt	Platelet
PSG	Polysomnography
QC	Quality Control
ROC	Receiver Operating Characteristic
ROS	Reactive Oxygen Species
SCFAs	Short Chain Fatty Acids
SF	Sleep Fragmentation
TC	Total Cholesterol
TG	Triglyceride
UA	Uric Acid
VIP	Variable Importance in Projection

Supplementary Information

The online version contains supplementary material available at <https://doi.org/10.1186/s12887-025-05561-4>.

Supplementary Material 1

Acknowledgements

We thank all the children and their parents who participated in this study. We thank the Science and Technology Projects of Medicine and Health of Zhejiang (No. 2024KY1576), Ningbo key discipline Pediatrics (No. 2022-B17), the Ningbo Clinical Research Center for Children's Health and Diseases (No. 2019A21002), the Innovation Project of Distinguished Medical Team in Ningbo (No. 2022020405) and the Ningbo Medical and Health Brand Discipline (No. PPXK2024-06) for funding for this research.

Author contributions

Yanbo Lu collected data and carried out the initial analyses and drafted the initial manuscript. Junhua Wu conceived and designed the study and reviewed and revised the manuscript. Daina Chen completed most of the experiments and supervised the data analyses. Jishan Zheng coordinated and critically reviewed the manuscript for important intellectual content. All authors approved the final manuscript as submitted and agree to be accountable for all aspects of the work.

Funding

This study was supported by the Science and Technology Projects of Medicine and Health of Zhejiang (No. 2024KY1576), Ningbo key discipline Pediatrics (No. 2022-B17), the Ningbo Clinical Research Center for Children's Health and Diseases (No. 2019A21002) and the Innovation Project of Distinguished Medical Team in Ningbo (No. 2022020405) and the Ningbo Medical and Health Brand Discipline (No. PPXK2024-06).

Data availability

All raw data can be obtained by contacting the corresponding author.

Declarations

Ethics approval

The study was approved by the ethics committee of the affiliated Women and Children's Hospital of Ningbo University (no. EC2020-047) and carried out in accordance with the Helsinki Declaration.

Consent to participate

Written informed consent was obtained from the parents.

Consent to publish

Not applicable.

Competing interests

The authors declare no competing interests.

Received: 12 March 2024 / Accepted: 2 March 2025

Published online: 17 March 2025

References

1. Rundo JV. Obstructive sleep apnea basics [J]. *Cleve Clin J Med*. 2019;86(9 Suppl 1):2–9.
2. Kitamura T, Miyazaki S, Kadohira H, et al. Prevalence of obstructive sleep apnea syndrome in Japanese elementary school children aged 6–8 years [J]. *Sleep Breath*. 2014;18(2):359–66.
3. Li AM, So HK, Au CT, et al. Epidemiology of obstructive sleep Apnoea syndrome in Chinese children: a two-phase community study [J]. *Thorax*. 2010;65(11):991–7.
4. Tan HL, Gozal D, Kheirandish-Goza L. Obstructive sleep apnea in children: a critical update [J]. *Nat Sci Sleep*. 2013;25:5:109–23.
5. Lo Bue A, Salvaggio A, Insalaco G. Obstructive sleep apnea in developmental age. A narrative review [J]. *Eur J Pediatr*. 2020;179(3):357–65.
6. Li HY, Lee LA. Sleep-disordered breathing in children [J]. *Chang Gung Med J*. 2009;32(3):247–57.
7. Xin Ni Z, Gao D, Han, et al. Chinese guideline for the diagnosis and treatment of childhood obstructive sleep apnea (2020). *Chin J Otorhinolaryngol Head Neck Surg*. 2020;55(8):729–47.
8. De Luca Canto G, Pacheco-Pereira C, Aydinov S, et al. Biomarkers associated with obstructive sleep apnea and morbidities: a scoping review [J]. *Sleep Med*. 2015;16(3):347–57.

9. Kheirandish-Gozal L, Gozal D. Pediatric, OSA Syndrome Morbidity Biomarkers. *Hunt Is Finally [J]*. *Chest*. 2017;151(2):500–6.
10. Valentini F, Evangelisti M, Arpinelli M, et al. Gut microbiota composition in children with obstructive sleep Apnoea syndrome: a pilot study [J]. *Sleep Med*. 2020;76:140–7.
11. Wang F, Liu Q, Wu H, et al. The dysbiosis gut microbiota induces the alternation of metabolism and imbalance of Th17/Treg in OSA patients [J]. *Arch Microbiol*. 2022;23(4):217.
12. Collado MC, Katila MK, Vuorela NM, et al. Dysbiosis in snoring children: an interlink to comorbidities [J]? *J Pediatr Gastroenterol Nutr*. 2019;68(2):272–7.
13. Wu J, Lu Y, Cai X, et al. Gut microbiota dysbiosis in 4- to 6-year-old children with obstructive sleep apnea-hypopnea syndrome [J]. *Pediatr Pulmonol*. 2022;57(9):2012–22.
14. Ko CY, Liu QQ, Su HZ et al. Gut microbiota in obstructive sleep apnea-hypopnea syndrome: disease-related dysbiosis and metabolic comorbidities [J]. *Clin Sci (Lond)*. 2019;123(7):905–917.
15. O'Connor KM, Lucking EF, Golubeva AV, et al. Manipulation of gut microbiota blunts the ventilatory response to hypercapnia in adult rats [J]. *EBioMedicine*. 2019;44:618–38.
16. Dong Y, Wang P, Lin J, et al. Characterization of fecal metabolome changes in patients with obstructive sleep apnea [J]. *J Clin Sleep Med*. 2022;18(1):575–86.
17. Jo J, Gavrilova O, Pack S, et al. Hypertrophy and/or hyperplasia: dynamics of adipose tissue growth [J]. *PLoS Comput Biol*. 2009;5(3):e1000324.
18. Almendros I, Martinez-Garcia MA, Farré R, et al. Obesity, sleep apnea, and cancer [J]. *Int J Obes (Lond)*. 2020;44(8):1653–67.
19. Dosman JA, Karunanayake CP, Fenton M, et al. Obesity, sex, snoring and severity of OSA in a first Nation community in Saskatchewan, Canada [J]. *Clocks Sleep*. 2022;24(1):100–13.
20. Bachrach K, Danis DO 3rd, Cohen MB, et al. The relationship between obstructive sleep apnea and pediatric obesity: A nationwide analysis [J]. *Ann Otol Rhinol Laryngol*. 2022;131(5):520–6.
21. Orrù G, Storari M, Scano A, et al. Obstructive sleep apnea, oxidative stress, inflammation and endothelial dysfunction—An overview of predictive laboratory biomarkers [J]. *Eur Rev Med Pharmacol Sci*. 2020;24(12):6939–48.
22. Meszaros M, Bikov A. Obstructive sleep Apnoea and lipid metabolism: the summary of evidence and future perspectives in the pathophysiology of OSA-Associated dyslipidaemia [J]. *Biomedicines*. 2022;10(1):29.
23. Maniacci A, Iannella G, Cocuzza S, et al. Oxidative stress and inflammation biomarker expression in obstructive sleep apnea patients [J]. *J Clin Med*. 2021;10(2):13.
24. Bhatt SP, Guleria R, Kabra SK. Metabolic alterations and systemic inflammation in overweight/obese children with obstructive sleep apnea [J]. *PLoS ONE*. 2021;4(6):e0252353.
25. Martelli V, Carelli E, Tomlinson GA, et al. Prevalence of elevated hemoglobin and hematocrit levels in patients with obstructive sleep apnea and the impact of treatment with continuous positive airway pressure: a meta-analysis [J]. *Hematology*. 2022;27(1):889–901.
26. Shen T, Wang J, Li L, et al. Changes in platelet count and coagulation parameters in children with obstructive sleep apnea [J]. *Sleep Breath*. 2022;26(2):871–8.
27. Zeng Z, Jin T, Ni J, et al. Assessing the causal associations of obstructive sleep apnea with serum uric acid levels and gout: a bidirectional two-sample Mendelian randomization study [J]. *Semin Arthritis Rheum*. 2022;57:152095.
28. Campos-Rodriguez F, Reyes-Núñez N, Queipo-Corona C, et al. Continuous positive airway pressure treatment does not reduce uric acid levels in OSA women [J]. *Arch Bronconeumol (Engl Ed)*. 2019;55(4):201–7.
29. Lin CH, Lurie RC, Lyons OD. Sleep apnea and chronic kidney disease: A State-of-the-Art. *Rev [J] Chest*. 2020;157(3):673–85.
30. Pochetti P, Azzolina D, Ragnoli B, et al. Interrelationship among obstructive sleep apnea, renal function and survival: A cohort study [J]. *Int J Environ Res Public Health*. 2020;17(14):8.
31. Tripathi A, Xu ZZ, Xue J et al. Intermittent hypoxia and hypercapnia reproducibly change the gut Microbiome and metabolome across rodent model systems [J]. *mSystems*. 2019, 30;4(2):e00058-19.
32. Ratajczak W, Rył A, Mizerski A, et al. Immunomodulatory potential of gut microbiome-derived short-chain fatty acids (SCFAs) [J]. *Acta Biochim Pol*. 2019;66(4):1–12.
33. Dalile B, Van Oudenhove L, Vervliet B, Verbeke K. The role of short-chain fatty acids in microbiota-gut-brain communication [J]. *Nat Rev Gastroenterol Hepatol*. 2019;16(8):461–78.
34. Schönfeld P, Wojtczak L. Short- and medium-chain fatty acids in energy metabolism: the cellular perspective [J]. *J Lipid Res*. 2016;57(6):943–54.
35. Li X, Zhou W, Zhuang Y, et al. Biosynthesis of 3,4-dihydroxymandelic acid in *Escherichia coli* [J]. *Biotechnol Bull*. 2017;01:135–40.
36. Sule N, Pasupuleti S, Kohli N, et al. The norepinephrine metabolite 3,4-Dihydroxymandelic acid is produced by the commensal microbiota and promotes chemotaxis and virulence gene expression in enterohemorrhagic *Escherichia coli* [J]. *Infect Immun*. 2017;20(10):e00431–17.
37. Ley JP, Engelhart K, Bernhardt J, et al. 3,4-Dihydroxymandelic acid, a Nor-adrenalin metabolite with powerful antioxidative potential [J]. *J Agric Food Chem*. 2002;9(21):5897–902.
38. Prabhakar NR, Peng YJ, Nanduri J. Hypoxia-inducible factors and obstructive sleep apnea [J]. *J Clin Invest*. 2020;130(1):5042–51.
39. Hoshino H, Tanooka H. Carcinogenicity of triethanolamine in mice and its mutagenicity after reaction with sodium nitrite in bacteria [J]. *Cancer Res*. 1978;38(11 Pt 1):3918–21.
40. Milanesi N, Berti S, Gola M. Allergic contact dermatitis to triethanolamine in a child [J]. *Pediatr Dermatol*. 2015;32(3):e112–3.
41. Herman JJ. Intractable sneezing due to IgE-mediated triethanolamine sensitivity [J]. *J Allergy Clin Immunol*. 1983;71(3):339–44.
42. Gamer AO, Rossbacher R, Kaufmann W, et al. The inhalation toxicity of di- and triethanolamine upon repeated exposure [J]. *Food Chem Toxicol*. 2008;46(6):2173–83.
43. Garabadzhiu AV, Voronkov MG, Nyanikova GG, et al. The influence of silatrane, geratranes, protatranes, and triethanolamine on vital functions of microorganisms [J]. *Dokl Biol Sci*. 2011;439:264–6.
44. Liu X, Bian L, Duan X, et al. Alantolactone: A sesquiterpene lactone with diverse Pharmacological effects [J]. *Chem Biol Drug Des*. 2021;98(6):1131–45.
45. Stojanović-Radić Z, Comić L, Radulović N, et al. Antistaphylococcal activity of *Inula helenium* L. root essential oil: Eudesmane sesquiterpene lactones induce cell membrane damage [J]. *Eur J Clin Microbiol Infect Dis*. 2012;31(6):1015–25.
46. Gierlikowska B, Gierlikowski W, Bekier K, et al. *Inula helenium* and *Grindelia squarrosa* as a source of compounds with anti-inflammatory activity in human neutrophils and cultured human respiratory epithelium [J]. *J Ethnopharmacol*. 2020;249:1.
47. Seca AM, Grigore A, Pinto DC, et al. The genus *Inula* and their metabolites: from ethnopharmacological to medicinal uses [J]. *J Ethnopharmacol*. 2014;11(2):286–310.
48. Gao S, Wang Q, Tian XH, et al. Total sesquiterpene lactones prepared from *Inula helenium* L. has potentials in prevention and therapy of rheumatoid arthritis [J]. *J Ethnopharmacol*. 2017;20:19639–46.
49. Kim M, Song K, Kim YS. Alantolactone improves palmitate-induced glucose intolerance and inflammation in both lean and obese States in vitro: adipocyte and adipocyte-macrophage co-culture system [J]. *Int Immunopharmacol*. 2017;49:187–94.
50. Kim M, Song K, Kim YS. Alantolactone improves prolonged exposure of Interleukin-6-Induced skeletal muscle inflammation associated glucose intolerance and insulin resistance [J]. *Front Pharmacol*. 2017;8:29.
51. Yang M, Zhao H, Ai H, et al. Alantolactone suppresses APOC3 expression and alters lipid homeostasis in L02 liver cells [J]. *Eur J Pharmacol*. 2018;5:828:60–6.
52. Wang X, Lan YL, Xing JS, et al. Alantolactone plays neuroprotective roles in traumatic brain injury in rats via anti-inflammatory, anti-oxidative and anti-apoptosis pathways [J]. *Am J Transl Res*. 2018;15(2):368–80.
53. Mengsha Cen Y, Zhu Y, Shen, et al. Mechanism study on the imbalance of gut microbiota mediated by deoxycholic acid and abnormal bile acid metabolism promoting the occurrence and development of enteritis [J]. *Chin J Inflamm Bowel Disease*. 2021;01:77–83.
54. Jairajpuri DS, Jairajpuri ZS. Isoferulic acid action against Glycation-Induced changes in structural and functional attributes of human High-Density lipoprotein [J]. *Biochem (Mosc)*. 2016;81(3):289–95.
55. Hirabayashi T, Ochiai H, Sakai S, et al. Inhibitory effect of ferulic acid and isoferulic acid on murine interleukin-8 production in response to influenza virus infections in vitro and in vivo [J]. *Planta Med*. 1995;61(3):221–6.
56. Sakai S, Kawamata H, Kogure T, et al. Inhibitory effect of ferulic acid and isoferulic acid on the production of macrophage inflammatory protein-2 in response to respiratory syncytial virus infection in RAW264.7 cells [J]. *Mediators Inflamm*. 1999;8(3):173–5.
57. Liu IM, Hsu FL, Chen CF, et al. Antihyperglycemic action of isoferulic acid in streptozotocin-induced diabetic rats [J]. *Br J Pharmacol*. 2000;129(4):631–6.

58. Liu IM, Chen WC, Cheng JT. Mediation of beta-endorphin by isoferulic acid to lower plasma glucose in streptozotocin-induced diabetic rats [J]. *J Pharmacol Exp Ther*. 2003;307(3):1196–204.
59. Muraki I, Wada H, Tanigawa T. Sleep apnea and type 2 diabetes [J]. *J Diabetes Investig*. 2018;9(5):991–7.
60. Machado Dutra J, Espitia PJP, Andrade Batista R, Formononetin. Biological effects and uses - A review [J]. *Food Chem*. 2021;359:15.

Publisher's note

Springer Nature remains neutral with regard to jurisdictional claims in published maps and institutional affiliations.